

# The morphology and kinematics of the Fine Ring Nebula, planetary nebula Sp 1, and the shaping influence of its binary central star<sup>\*</sup>

D. Jones<sup>1†</sup>, D. L. Mitchell<sup>2,3</sup>, M. Lloyd<sup>3</sup>, D. Pollacco<sup>4</sup>, T. J. O’Brien<sup>3</sup>, J. Meaburn<sup>3</sup> and N. M. H. Vaytet<sup>5</sup>

<sup>1</sup>*European Southern Observatory, Alonso de Córdova 3107, Casilla 19001, Santiago, Chile*

<sup>2</sup>*Chalmers Tekniska Högskola, SE-412 96 Gothenburg, Sweden*

<sup>3</sup>*Jodrell Bank Centre for Astrophysics, School of Physics and Astronomy, University of Manchester, M13 9PL, UK*

<sup>4</sup>*Astrophysics Research Centre, Queen’s University Belfast, BT7 1NN, UK*

<sup>5</sup>*École Normale Supérieure de Lyon, CRAL (UMR CNRS 5574), Lyon, France*

Accepted . Received ; in original form

## ABSTRACT

We present the first detailed spatio-kinematical analysis and modelling of the planetary nebula Shapley 1 (Sp 1), which is known to contain a close-binary central star system. Close-binary central stars have been identified as a likely source of shaping in planetary nebulae, but with little observational support to date.

Deep narrowband imaging in the light of [O III]  $\lambda 5007$  Å suggests the presence of a large bow-shock to the west of the nebula, indicating that it is undergoing the first stages of an interaction with the interstellar medium. Further narrowband imaging in the light of  $H\alpha$ + [N II]  $\lambda 6584$  Å combined with longslit observations of the  $H\alpha$  emission have been used to develop a spatio-kinematical model of Sp 1. The model clearly reveals Sp 1 to be a bipolar, axisymmetric structure viewed almost pole-on. The symmetry axis of the model nebula is within a few degrees of perpendicular to the orbital plane of the central binary system - strong evidence that the central close-binary system has played an important role in shaping the nebula.

Sp 1 is one of very few nebulae to have this link, between nebular symmetry axis and binary plane, shown observationally.

**Key words:** planetary nebulae: individual: Sp 1 – planetary nebulae: PN G329.0+01.9 – circumstellar matter – stars: mass-loss – stars: winds, outflows – binaries: close

## 1 INTRODUCTION

Only a handful of planetary nebulae (PNe) are known to contain close-binary nuclei ( $\sim 40$ , de Marco 2009, Miszalski et al. 2009a, Miszalski et al. 2011a, Corradi et al. 2011, Miszalski et al. 2011b, Santander-García et al. 2011), yet it is widely believed that a close-binary central star is required to form an aspherical nebula (as the vast majority of PNe are). The relatively small number of PNe known to host a central binary system is thought to be more a reflection of the difficulty in their detection than an accurate representation of the total number of central binary stars.

The generalised interacting stellar winds model (Kwok et al. 1978; Kahn & West 1985; Balick & Frank 2002) has proven the most effective theory in explaining some of the morphologies seen in PNe. In this model, a slow, dense wind containing much of the envelope mass is blown at the end of the asymptotic giant branch (AGB) phase, and then swept up into a shell-like structure by a subsequent fast, tenuous wind from the emerging post-AGB star. In order to recreate aspherical PNe, the slow AGB wind is assumed to be equatorially enhanced. Only the effect of a close-binary partner is believed to provide the necessary equatorial enhancement to produce the most aspherical nebulae (magnetic fields have been considered, but cannot be sustained at the necessary levels for sufficient time to have the required effect, Nordhaus et al. 2007). While theoretical support for this “binary hypothesis” is abundant, observational evidence has been lacking. In order to address this,

<sup>\*</sup> Based on the observations made with European Southern Observatory telescopes at the La Silla or Paranal Observatories under programme IDs 74.D-0373 and 55.D-0550.

<sup>†</sup> E-mail: djones@eso.org

the PLaN-B working group<sup>1</sup> was formed to co-ordinate the investigative effort.

Spatio-kinematic modelling is an important tool in the testing of theoretical models, providing 3-D morphologies and orientations as well as the velocity field of the outflows and their kinematical ages, all of which must be replicated theoretically. Additionally, for those PNe with well constrained binary systems, one can compare the parameters of the central binaries to those of their host nebulae, in particular the theoretical prediction that the nebular symmetry axis will lie perpendicular to the orbital plane of the binary system (Nordhaus & Blackman 2006).

Sp 1 ( $\alpha = 15^h 51^m 41^s$ ,  $\delta = -51^\circ 31' 23''$ , J2000), discovered by Shapley (1936), was described as “nearly perfectly circular” in appearance by Bond & Livio (1990, see Fig. 1). This apparent morphology is somewhat at odds with presence of a binary central star, discovered spectroscopically by Méndez et al. (1988) and confirmed photometrically by Bond & Livio (1990), which would be expected to produce an aspherical nebula. However, this can be reconciled by the hypothesis that Sp 1 is actually an axisymmetric nebula viewed almost pole-on, making Sp 1 morphologically akin to other PNe with known close-binary central stars (A 63: Mitchell et al. 2007; A 41: Jones et al. 2010b; NGC6337: García-Díaz et al. 2009; HaTr 4: Tyndall et al. 2011b). This interpretation is “supported by the low amplitude of the photometric variations of the central star and the absence of an eclipse” (Bond & Livio 1990). Recent work by Bodman, Schaub & Hillwig (2011) and Hillwig et al. (in preparation) photometrically confirms the 2.9 day period of Bond & Livio 1990, and indicates that the binary plane does indeed lie very close to the plane of the sky ( $10^\circ \geq i \geq 20^\circ$ ).

Indeed, it has been proposed that many ring-like PNe may be bipolars with symmetry axes inclined to the plane of the sky; this suggestion is supported by kinematical studies of several ring-like PNe, all of which are found to be bipolar, e.g. the Ring Nebula (Bryce et al. 1994), LoTr 5 (Graham et al. 2004), the Helix Nebula (Meaburn et al. 2005), SBW 1 (Smith et al. 2007) and SuWt 2 (Jones et al. 2010a).

Despite the importance of Sp 1 as a test of current understanding of how close-binaries affect the morphological evolution of PNe, until now, there have been no kinematical observations of the nebula in order to constrain its three dimensional structure. Detailed imagery and high-resolution longslit spectroscopy are thus presented in order to determine the true morphology of Sp 1. The nebula morphology and orientation are then compared to that of the central binary in order to ascertain their relationship and test current theories of binary-induced PN shaping.

## 2 OBSERVATIONS

### 2.1 NTT observations

Deep narrow-band [O III]  $\lambda 5007 \text{ \AA}$  and  $\text{H}\alpha^3$  imagery of Sp 1 was obtained using the ESO (European Southern Observatory) Multi-Mode Instrument (EMMI; Dekker et al. 1986) on the 3.6-m ESO New Technology Telescope (NTT), and is shown in Fig. 1. The 1200-s [O III]  $\lambda 5007 \text{ \AA}$  image (Fig. 1(a)) was taken on 1995 April 22 with a seeing of  $1''$  and shows the nebula as a diffuse ring in the plane of the sky, upon which, bright filaments are superimposed. The filaments give the appearance of two bright, narrow rings. It is not clear whether they are two concentric rings or two rings that are offset in the east-west direction. The filaments appear to intersect in the south of the nebula, but there is no obvious counterpart in the north, which would be expected if they are two offset rings. Both rings are brighter in the west of the nebula than the east. Diffuse material is present in the innermost region of the nebula and a very faint outer “halo” is visible surrounding the bright nebular shell. The 900-s  $\text{H}\alpha$  image (Fig. 1(b)), taken on 2005 March 03 with a seeing of  $0.9''$ , shows the same bright ring-like filaments, however, the diffuse material visible close to the central star appears brighter in  $\text{H}\alpha$  than in [O III]  $\lambda 5007 \text{ \AA}$ .

The [O III]  $\lambda 5007 \text{ \AA}$  image is also shown at low-contrast in Fig. 1c to reveal, for the first time, a prominent bowshock to the west of Sp 1. The origin of this bowshock is discussed in Section 3.2.

Spatially resolved, longslit emission-line spectra of Sp 1 were been obtained with EMMI on the NTT. Observations took place in 2005 March 2-4 using the red arm of the spectrograph which employs two MIT/LL CCDs, each of  $2048 \times 4096 \text{ } 15 \text{ } \mu\text{m}$  pixels ( $\equiv 0.166''$  per pixel), in a mosaic. There is a gap of 47 pixels ( $\equiv 7.82''$ ) between the two CCD chips which can be seen in the observed spectra.

EMMI was used in single order echelle mode, with grating #10 and a narrow-band  $\text{H}\alpha$  filter (#596) to isolate the 87<sup>th</sup> echelle order containing the  $\text{H}\alpha$  and [N II]  $\lambda 6584 \text{ \AA}$  emission lines. Binning of  $2 \times 2$  was used giving spatial and spectral scales of  $0.33''$  per pixel and  $3.8 \text{ km s}^{-1}$  per pixel, respectively. The slit had a length of  $330''$  and width  $1''$  ( $\equiv 10 \text{ km s}^{-1}$ ). All integrations were of 1800 s duration and the seeing never exceeded  $1''$ .

Data reduction was performed using STARLINK software. The spectra were bias-corrected and cleaned of cosmic rays. The spectra were then wavelength calibrated against a long exposure ThAr emission lamp, taken at the start of each night. The calibration was confirmed using short Ne emission lamp exposures throughout the night, and by checking the wavelengths of skylines visible in the exposure. Finally the data were rescaled to a linear velocity scale (relative to the rest wavelength of  $\text{H}\alpha$  taken to be  $6562.81 \text{ \AA}$ ) and corrected for Heliocentric velocity.

Five slit positions were obtained with the slit orientated east-west across Sp 1 (numbered 1 to 5) and four slit positions with the slit positioned in a north-south direction (number 6 to 9). The slit positions are shown on the [O III]

<sup>1</sup> <http://www.wiyn.org/planb/>

<sup>2</sup> Here, the inclination,  $i$ , is defined such that for  $i = 90^\circ$  the orbital plane would be in the line of sight (i.e. eclipsing).

<sup>3</sup> The filter used also includes the [N II]  $\lambda 6584 \text{ \AA}$  emission line, but the spectroscopy described later confirms that Sp 1 displays almost no [N II]  $\lambda 6584 \text{ \AA}$  emission.

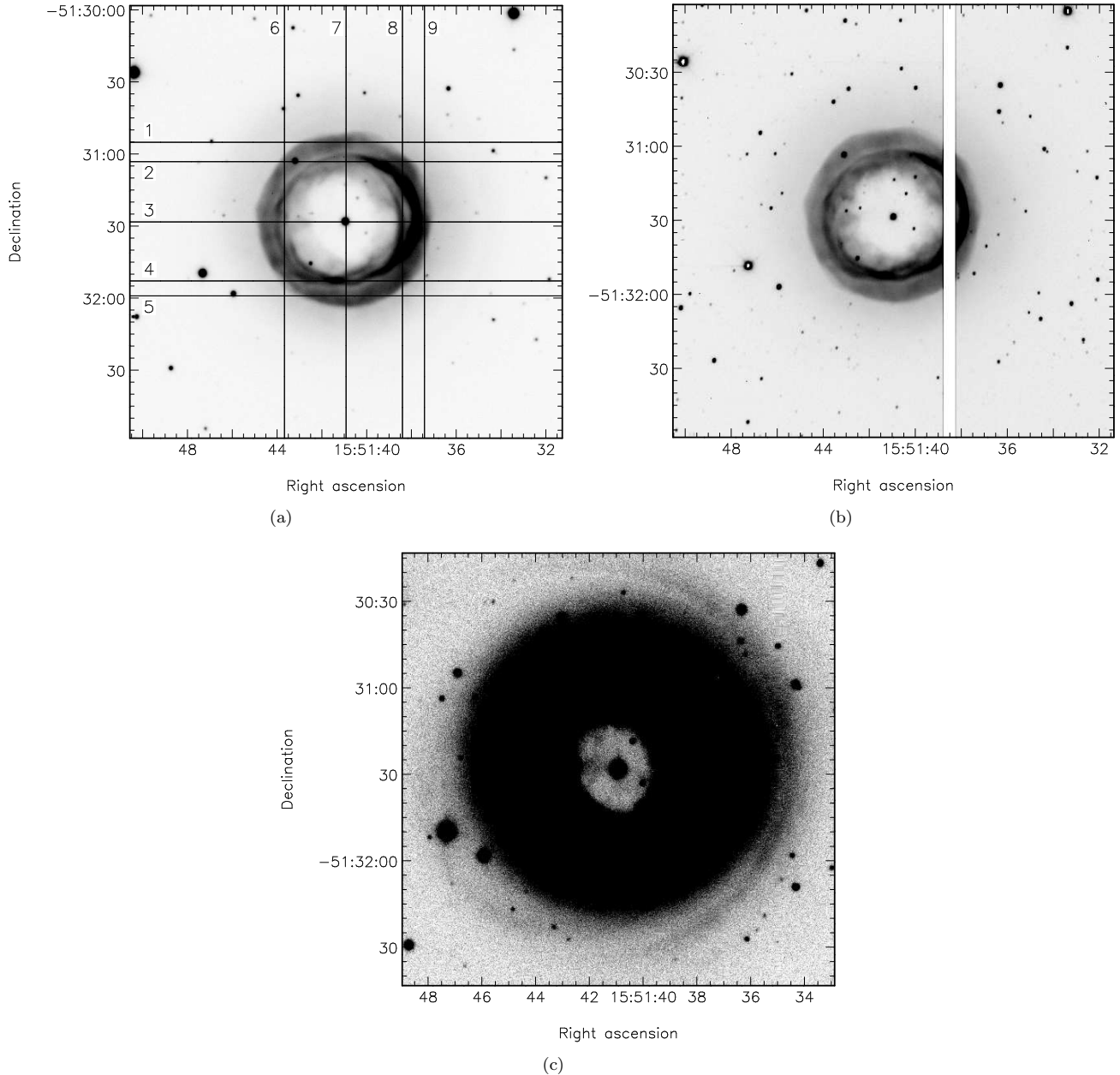


**Figure 1.** Narrowband EMMI-NTT images of Sp 1 at (a)  $[\text{O III}] \lambda 5007 \text{ \AA}$  (showing the observed slit positions) and (b)  $H\alpha$ . The vertical white stripe in the  $H\alpha$  image is a result of the overscan gap between the master and slave CCD chips. The lower panel (c) shows the  $[\text{O III}] \lambda 5007 \text{ \AA}$  image but at low contrast to reveal the faint bowshock to the west of the main nebula.

$\lambda 5007 \text{ \AA}$  image of Sp 1 in Fig. 1(a) (Note that the full  $6'$  extent of the slits is not shown). The fully reduced position-velocity (PV) arrays for  $H\alpha$  emission are shown in Fig. 2, respectively (as there is very little  $[\text{N II}] \lambda 6584 \text{ \AA}$  emission present, the spectra have been cropped to display  $H\alpha$  emission only).

## 2.2 AAT spectroscopy

Complementary longslit observations of Sp 1 were obtained using UCLES combined with the 3.9-m  $f/36$  AAT. UCLES was used in its primary spectral mode with a narrow-band filter to isolate the  $H\alpha + [\text{N II}] \lambda 6584 \text{ \AA}$  emission lines in

the 34th echelle order. Observations took place in January 2005 using an EEV2 CCD with  $2048 \times 4096$   $13.5 \mu\text{m}$  square pixels, but using a  $960 \times 4096$  subsection of the CCD ( $\equiv 0.16'' \text{ pixel}^{-1}$ ). All integrations were of 1800-s duration.

Binning of  $2 \times 3$  was adopted during the observations, giving 2096 pixels in the spectral (x) direction ( $\equiv 3.88 \text{ kms}^{-1} \text{ pixel}^{-1}$ ) and 320 pixels in the spatial (y) direction ( $\equiv 0.48'' \text{ pixel}^{-1}$ ). This gave a projected slit length of  $56.125''$  on the sky. The slit width was  $1.971''$  ( $\equiv 10 \text{ kms}^{-1}$ ).

Two integrations were obtained with the slit orientated north-south along the nebula,  $5''$  either side of the central star. Data reduction was performed in the same manner as for the EMMI spectra. Unfortunately the observations were

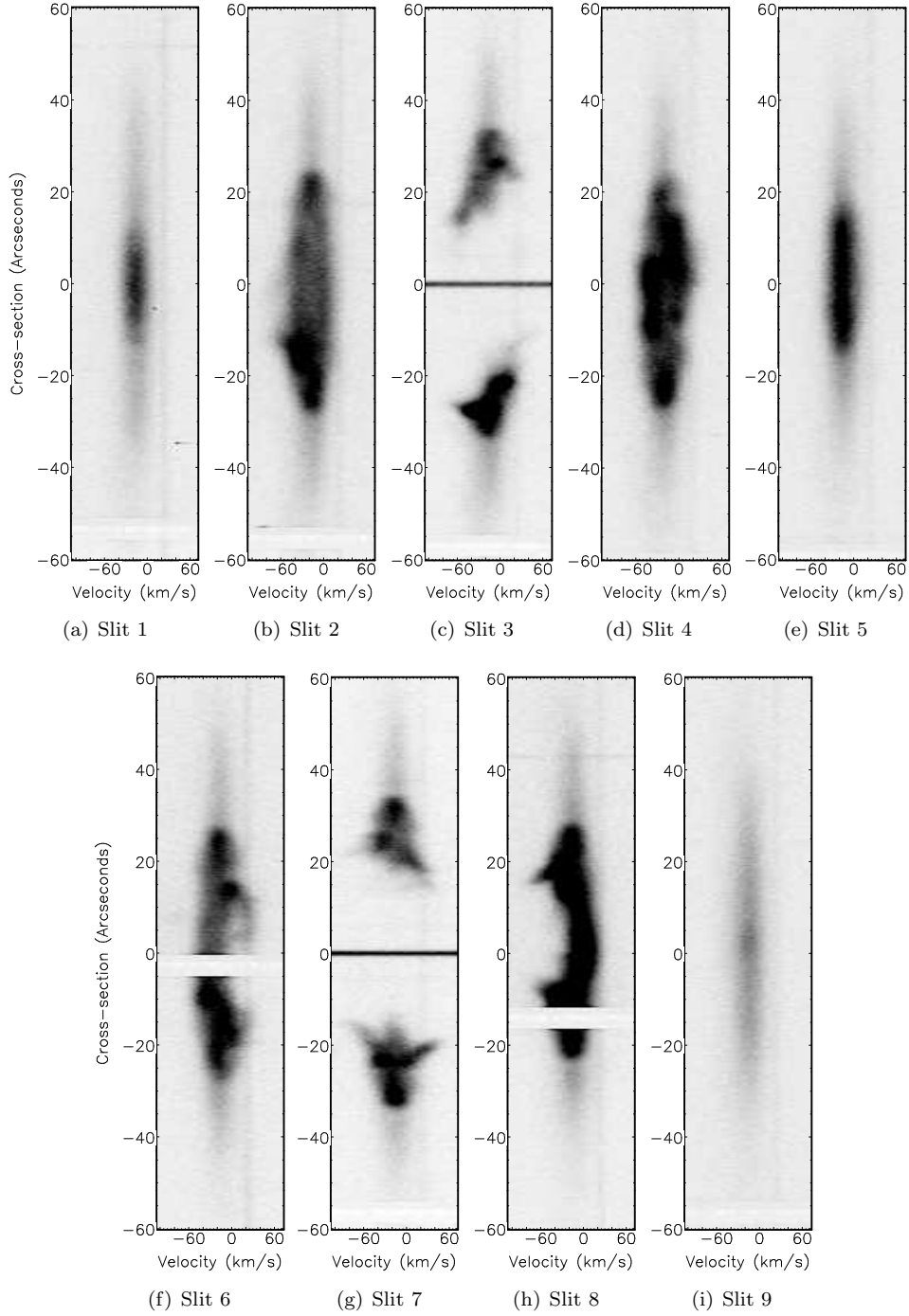


**Figure 2.**  $H\alpha$  longslit spectra of Sp 1 obtained with EMMI combined with the NTT. The slit positions are drawn on Fig. 1(a). Cross-section zero corresponds to the position of the central star and the velocity axis on all plots is heliocentric velocity,  $v_{hel}$ . The horizontal white stripes that appear in some of the spectra result from the overscan gap between the master and slave CCD chips.

limited due to poor weather, and hence full cuts across the nebula were not obtained (single slits did not extend across the entire diameter of Sp 1). The data are consistent with the MES-SPM data shown here, and are available for down-

load from The San Pedro Mártir Kinematic Catalogue of Galactic Planetary Nebulae<sup>4</sup> (López et al. 2012).

<sup>4</sup> <http://kincatpn.astrosen.unam.mx>

### 2.3 SAAO photometry

Based on the period and amplitude of the reflection effect discussed by Bond & Livio (1990), we performed preliminary modelling of the central binary of Sp 1 using the Wilson-Devinney formulation (Wilson & Devinney 1971). For a given primary component, the amplitude of the reflection effect is primarily governed by the size of the secondary component, the orbital period and inclination. Assuming a low orbital inclination (as suspected from the nebular imagery, Bond & Livio 1990), it was found that a secondary much larger than a main sequence M-dwarf is required to replicate the observations (just as found by Bodman, Schaub & Hillwig 2011). This is similar to the results determined for the eclipsing central stars of Abell 46 and Abell 63, V477 Lyrae and UU Sge (Pollacco & Bell 1993, 1994). For orbital inclinations lower than  $\sim 15^\circ$ , we found that an M-dwarf secondary would need to be very close to filling its Roche lobe in order to replicate the reported period and amplitude of Sp 1.

High cadence photometry was acquired in order to look for signs of on-going mass transfer, from a Roche lobe filling secondary onto the primary, in the central star of Sp 1. The central star of Sp 1 was observed in consecutive 90-s exposures in the I-band for between 1 and 3 hours on the nights of 2010 March 24, 25, 27, 28, 29, 31 and April 1, 2 and 6 using the SAAO CCD on the 1.9-m Radcliffe Telescope of the South African Astronomical Observatory (SAAO). The SAAO CCD was employed with a SITe4 CCD binned  $2 \times 2$  resulting in a pixel scale of  $0.28''$  per pixel. The seeing during the observations varied between  $1''$  and  $4''$ . The resulting data were debiased and flat-fielded using standard STARLINK routines.

Differential photometry of the central star, with respect to a non-variable field star, was performed using SEXTRACTOR (Bertin 1997) with photometric aperture of radius equal to  $1.5 \times$  the seeing of each individual frame. Due to the roughly 3 day period of the variability the resulting lightcurve is highly fragmentary (and as a result is not presented here), but entirely consistent with the 2.91 day period determined by Bond & Livio (1990). No evidence for further short-timescale variability, which would be consistent with on-going accretion was found. Further detailed study of the central star system (such as that of Hillwig et al. in prep.), including spectroscopic observations, is required to fully constrain the Roche lobe filling factor of the secondary.

## 3 ANALYSIS

### 3.1 Longslit spectroscopy

All longslit spectra are bright in  $H\alpha$  and the nebular shell is also faintly visible in  $\text{He II } \lambda 6560 \text{ \AA}$  emission. A longslit spectrum (from slit position 7) is shown at low contrast in Fig. 3 to reveal the  $\text{He II } \lambda 6560 \text{ \AA}$  emission. The  $\text{He II } \lambda 6560 \text{ \AA}$  emission emanates from the bright nebular shell and ring-like filaments of Sp 1, but no  $\text{He II } \lambda 6560 \text{ \AA}$  emission is visible from the faint, outer “halo”. The presence of  $\text{He II } \lambda 6560 \text{ \AA}$  and absence of  $[\text{N II}] \lambda 6584 \text{ \AA}$  emission indicates that Sp 1 is a high excitation nebula with a very hot central star, entirely consistent with the temperature determined by Frew (2008) of 72,000 Kelvin using the Zanstra Method.

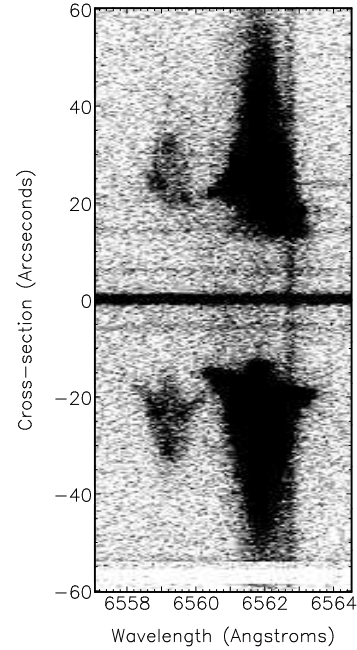


**Figure 3.**  $H\alpha$  longslit spectrum (slit position 7) shown at low contrast in order to reveal the faint  $\text{He II } \lambda 6560 \text{ \AA}$  emission. The  $\text{He II } \lambda 6560 \text{ \AA}$  emission reflects the velocity structure of the  $H\alpha$  line. The  $H\alpha$  airglow line is present at  $6562.817 \text{ \AA}$ .

The PV array from Slit 3 (Fig. 2(c)), which is orientated east-west (at a position angle, PA, of  $-90^\circ$ ) and crosses the central star of Sp 1, shows two bright emission regions corresponding to the east and west of the nebular shell. These two regions are not joined in a velocity ellipse, indicating that Sp 1 is aspherical and open-ended. Both emission regions show a “chicken foot”-like profile with three spurs of emission directed towards the stellar continuum. These three spurs can be attributed to the approaching lobe (blue-shifted spur), waist region (central spur) and receding lobe (red-shifted spur) of a bipolar shell. Assuming an axisymmetric structure, the PV array also indicates that the nebular symmetry axis is probably inclined to the line of sight, as for an inclination of  $0^\circ$  one would expect the PV array to be mirror symmetric about the central star. As this is not the case, one can infer that the approaching lobe of the nebula is shifted to the east with respect to its receding counterpart (i.e. the blue-shifted spurs appear at more negative cross-sections than the corresponding red-shifted spurs).

The emission from Slit 7 (Fig. 2(g)), which runs north-south (at a PA of  $0^\circ$ ) and crosses the central star, displays a very similar “chicken foot” structure to the PV array from Slit 3 but without any obvious angular offset between blue- and red-shifted components. This indicates that the small deviation of the nebular symmetry axis, from the line-of-sight, is almost entirely in the east-west direction. This is confirmed by the PV arrays from Slits 2 and 4 (Figs. 2(b) & (d) crossing the north and south of the nebula, respectively, both at a PA of  $-90^\circ$ ), which both display velocity ellipses at roughly the same  $V_{hel}$ .

Slit positions 1 and 5 are positioned east-west across the large, diffuse nebular shell and slit position 9 is orientated north-south along the shell (see Fig. 1(a)). None of these slit

positions intersect with the bright nebular shell. The PV arrays from these Slits all show consistent velocity trends with a single velocity component centred on  $-18 \text{ km s}^{-1}$ . All of the longslit spectra contain faint extended emission at this velocity, forming a filled ellipse in the PV arrays, indicative that this emission originates from a filled “halo” surrounding the brighter nebular shell rather than a hollow second shell.

### 3.2 Interaction with the ISM

The presence of the bowshock in the deep [O III]  $\lambda 5007 \text{ \AA}$  image of Sp 1 indicates that it is undergoing an interaction with the surrounding interstellar medium (ISM), where the western side of the nebula is at the leading edge of its motion through the ISM. However, as no proper motion measurements exist for this nebula it is not possible to confirm its direction of motion relative to that of the local ISM (assumed to be due to Galactic rotation, as in the analysis of HFG 1 - another PN with a binary central star - performed by Meaburn et al. 2009). The bowshock places Sp 1 at stage 1 in the scheme of Wareing et al. (2007), meaning that this interaction with the ISM cannot explain why the nebular shell appears brighter in the west than the east. Any material to the west of the bowshock is expected to be compressed and appear brighter, whilst material to the east of the bowshock (including the nebular shell) will remain unperturbed (Wareing et al. 2007).

## 4 THE MORPHO-KINEMATICS OF SP 1

### 4.1 Spatio-kinematical modelling

A spatio-kinematical model, corresponding to the simplest three-dimensional structure consistent with the large-scale nebular  $\text{H}\alpha$  emission features, has been constructed for Sp 1. The modelling was performed in order to confirm the axisymmetric nature of the nebula and to constrain the inclination of this symmetry axis for comparison with the inclination of the central binary. The model was developed using NOVACART (Gill & O’Brien 1999) and assuming radial expansion (where the expansion velocity is proportional to distance from the nebular centre, commonly known as a Hubble-type flow). The scale of the flow was set by the maximum observed velocity between red- and blue-shifted components in the nebular PV arrays (Fig. 2), measured to be  $110 \text{ km s}^{-1}$ , indicating that the maximum expansion velocity at the tip of each lobe is  $\sim 55 \text{ km s}^{-1}$ . The systemic velocity of the nebula,  $V_{sys} = -18 \text{ km s}^{-1}$ , was set by the centroid of the faint extended emission attributed to the “halo” in Section 3. The other model parameters (e.g. dimensions and inclination) were manually varied over a wide range of values and the results compared by eye to both spectral observations and imagery, until a best fit was found.

The final model comprises an open-ended bipolar shell (with major to minor axis ratio of roughly 2:1) embedded in a filled spherical shell. The velocity of the filled, outer sphere was also proportional to radius with a maximum velocity of  $20 \text{ km s}^{-1}$ , and its density was set to half that of the offset ellipsoids to replicate the brightness contrast observed in Fig. 1. A two-dimensional image of the model viewed in

cross-section at an inclination of  $90^\circ$  is shown in Fig. 4a. Sp 1 was found to have an inclination in the range  $10^\circ$ – $15^\circ$ , and the model is shown at inclinations  $15^\circ$  and  $10^\circ$  in Figs. 4b and c, respectively.

The model successfully reproduces the two bright, offset rings and the larger diffuse ring when viewed at inclinations of  $10^\circ$  and  $15^\circ$ . Both models also reproduce the faint emission observed inside of the bright rings. The  $10^\circ$  model reproduces the observed offset between the two rings most convincingly.

The model is axisymmetric and therefore does not reproduce the difference in brightness observed between the east and west sides of Sp 1. The purpose of the model is simply to reproduce the large-scale velocity features observed in the longslit spectra of Sp 1.

Synthetic spectra extracted from both the  $10^\circ$  and  $15^\circ$  models coinciding with slit positions 3, 4, 6, 7 and 8 are shown in Figs. 5. Synthetic spectra from the other slit positions are not shown as the selected slits are sufficient to show the quality of fit provided by the model at the two inclinations.

The synthetic spectra extracted from the  $10^\circ$  model (Fig. 5) convincingly replicate the broad velocity characteristics observed at all slit positions. The synthetic spectra from positions 3 and 7 successfully reproduce the line splitting into three velocity components as observed in the  $\text{H}\alpha$  longslit spectra; however, the velocity of each component in the synthetic spectra does not fan out to higher velocities as markedly as in the observations. The accurate reproduction of the central spur of emission from both positions 3 and 7 is clear evidence of the bipolar shell’s pinched waist, as a more elliptical structure would only reproduce the red-shifted and blue-shifted spurs.

The synthetic spectrum from slit position 6 reproduces the red-shifted velocity ellipse, which is present in the  $\text{H}\alpha$  spectrum. The synthetic spectrum extracted from slit position 8 successfully reproduces the incomplete blue-shifted velocity ellipse.

In general, the synthetic spectra extracted from the model viewed at  $15^\circ$  (Fig. 5) resemble the observed velocity trends in the NTT longslit spectra more closely than the  $10^\circ$  model. At this inclination, the synthetic spectrum from slit position 3 reflects the tilted structure observed in the  $\text{H}\alpha$  spectrum and the synthetic spectrum from slit position 4 demonstrates a greater offset between the bright red- and blue-shifted filaments, which is in close agreement with the  $\text{H}\alpha$  spectrum. Only the synthetic spectrum from slit position 6 fails to convincingly model the observed spectrum at an inclination of  $15^\circ$ ; the synthetic spectrum does not form a complete red-shifted velocity ellipse as seen in the NTT  $\text{H}\alpha$  spectrum.

Overall, both  $10^\circ$  and  $15^\circ$  models satisfactorily reproduce the observed images and spectra, with the  $15^\circ$  model providing a better fit to the spectroscopy and the  $10^\circ$  model a better fit to the imagery. We, therefore, favour a nebular inclination between  $10^\circ$ – $15^\circ$ .

Comparison of both models with the observations shows no evidence for deviation from homologous expansion (Hubble-type flow) nor for any additional turbulent broadening in the nebular shell. The modelling clearly proves that Sp 1 exhibits an hourglass-like morphology with a well-

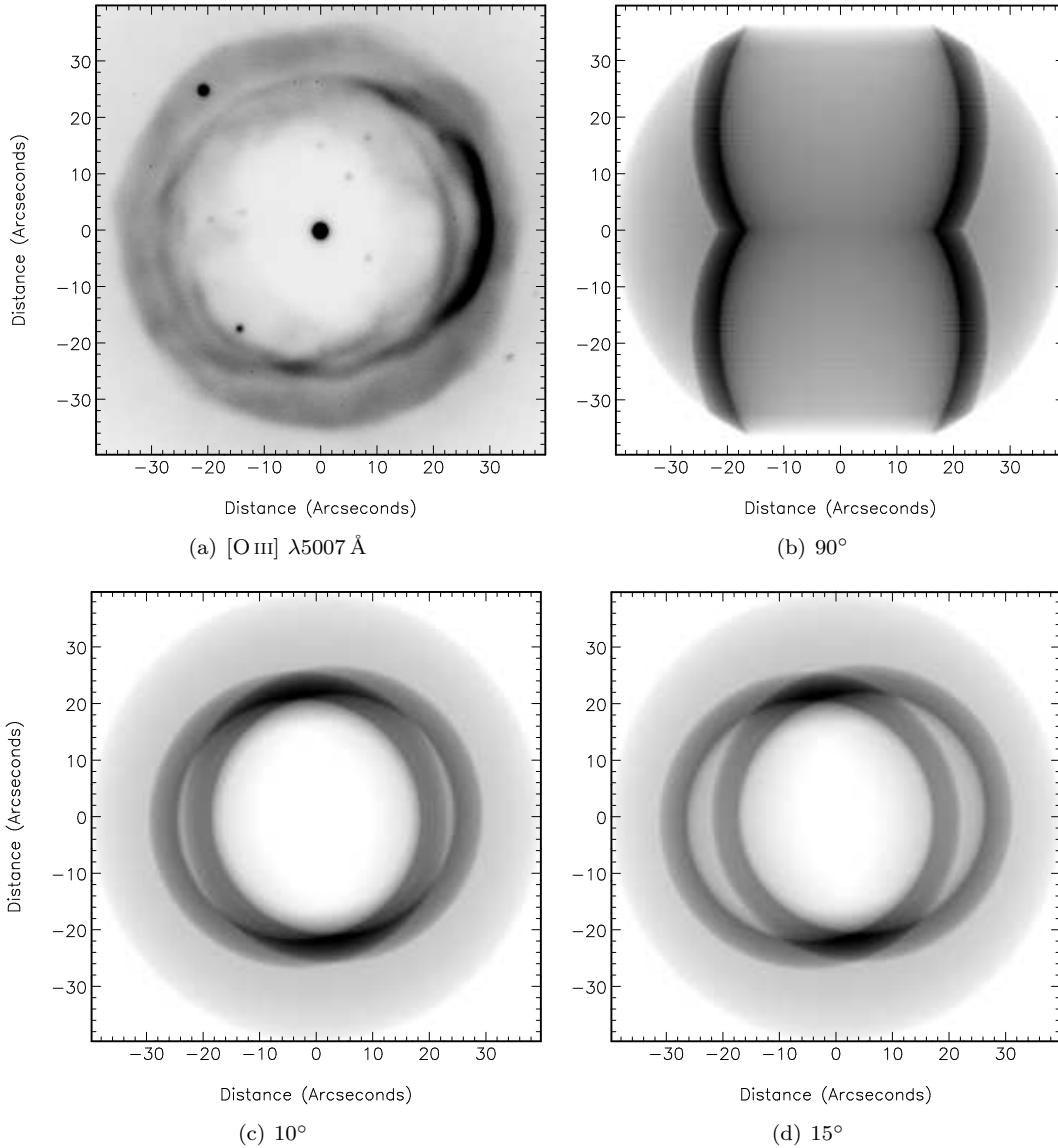


**Figure 4.** The observed [O III]  $\lambda 5007 \text{ \AA}$  image of Sp 1 (a) alongside two-dimensional grey-scale images of the morphological-kinematical model viewed at (b)  $90^\circ$ , (c)  $10^\circ$  and (d)  $15^\circ$ . The model nebula consists of a bright hourglass-shaped structure, embedded in a fainter “halo” (surrounding the waist of the nebula but not extending as far as the poles).

defined waist - no other morphology would be consistent with both the spectroscopy and imagery presented here.

#### 4.2 Kinematical age and systemic velocity

The radial velocities produced by both the  $10^\circ$  and  $15^\circ$  spatio-kinematical models accurately reflect those observed in the  $H\alpha$  longslit spectra. This suggests that the adopted maximum expansion velocities of  $55 \text{ km s}^{-1}$  for the ellipsoids and  $20 \text{ km s}^{-1}$  for the faint, surrounding sphere are very good approximations. The heliocentric systemic velocity of the model PN is  $-18 \pm 5 \text{ km s}^{-1}$ , somewhat at odds with the value of  $-31 \pm 3 \text{ km s}^{-1}$  determined by Meatheringham et al. (1988). No reasonable explanation could be found for this discrepancy - spectra from slits 3

and 5, which cross the nebular centre, were collapsed and then fitted with a gaussian profile following the method of Meatheringham et al. (1988) determining a value consistent with that taken from the spatio-kinematical modelling. To ensure that this was not an instrumental issue, the systemic velocity was confirmed using two UCLES spectra (Section 2.2), again following the same method used by Meatheringham et al. (1988).

The angular extent of the synthetic spectra is consistent with the observed spectra, which suggests the adopted geometrical dimensions in the model are also very good approximations. The angular distance between the ends of both lobes is  $\sim 70''$  (Fig. 4b). Adopting a distance to Sp 1 of  $1.5 \text{ kpc}$  (Sabbadin 1986) gives a physical distance between

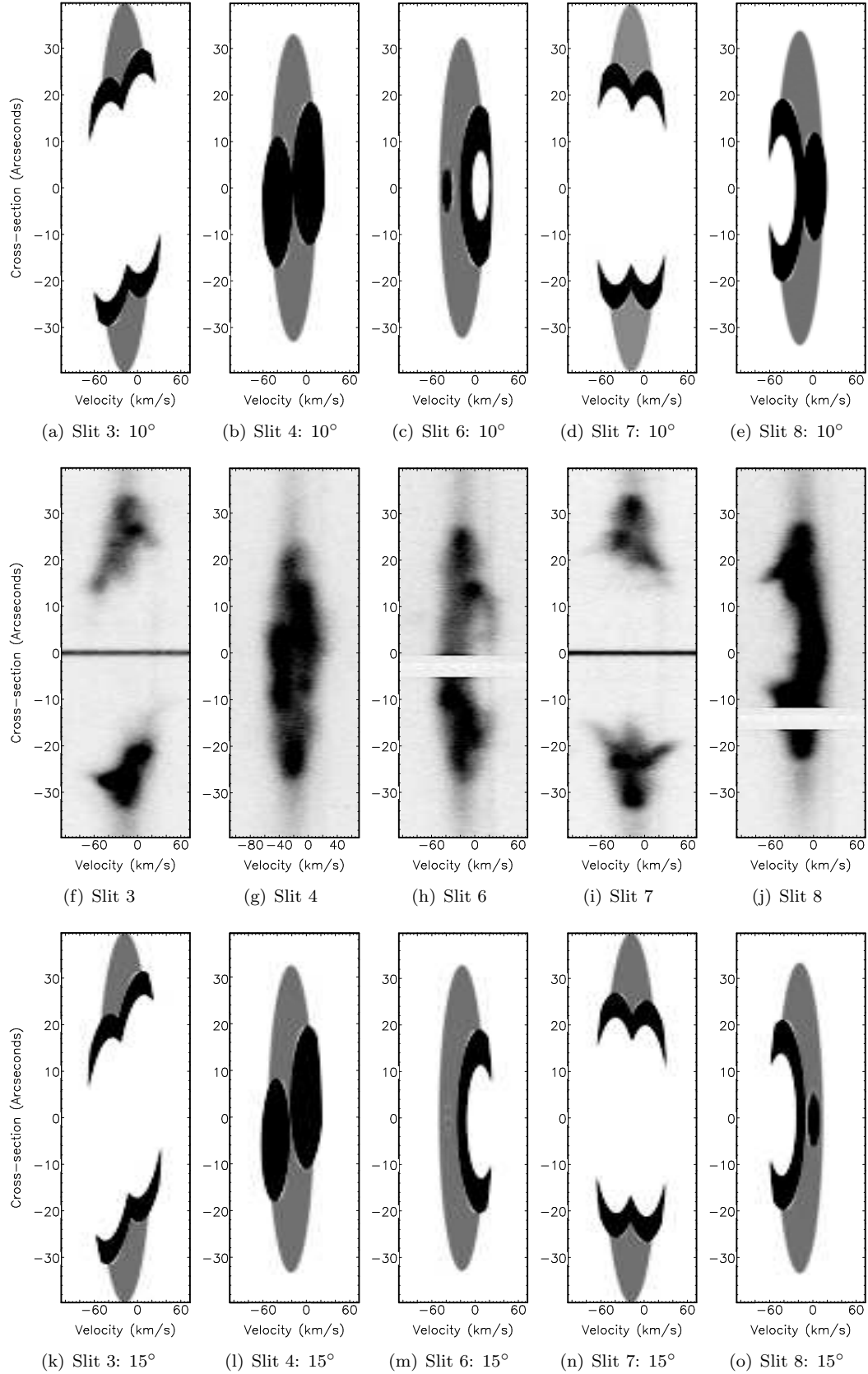


**Figure 5.** Synthetic spectra extracted from the morphological-kinematical model of Sp 1 viewed at an inclination of  $10^\circ$  (top) and  $15^\circ$  (bottom), alongside the corresponding  $H\alpha$  longslit spectra shown at the same scale for comparison (middle).



the ends of both lobes of 0.5 parsecs and a kinematical age of  $\sim 8700$  years.

## 5 DISCUSSION

High spatial and spectral resolution long-slit  $H\alpha$  spectra have been obtained from the Fine Ring Nebula, Sp 1. These spectra, together with deep narrow-band imagery, have been used to derive a spatio-kinematic model of the nebula proving its bipolar nature. The spatio-kinematical model of Sp 1 fits with the classical ‘butterfly’ morphology for a PN defined in the classification scheme of Balick (1987). The symmetry axis of the nebula is inclined almost along the line of sight ( $10^\circ \geq i \geq 15^\circ$ ). A Hubble-type flow is assumed with an equatorial expansion velocity of  $\sim 25 \text{ km s}^{-1}$ , consistent with typical PNe expansion velocities. The heliocentric velocity of the PN was found to be  $-18 \pm 5 \text{ km s}^{-1}$ . The kinematical age of Sp 1, at a distance of 1.5 kpc (Sabbadin 1986), is found to be  $\sim 8700$  years - well within the range of typical PN ages.

Sp 1 does *not* exhibit an exceptional morphology amongst the known sample of PNe with close-binary central stars. The bipolar structure of the main nebula is fairly prevalent amongst other PNe with binary central stars that have also been subjected to detailed spatio-kinematical modelling (Jones et al. 2011a,b). The faint sphere of material which surrounds the bipolar shell, referred to in the text as a “halo”, does not encompass the entire inner nebula, appearing mainly outside the waist of the bipolar shell. It is, therefore, possible that the “halo” is more akin to an equatorial enhancement (such as the one in seen in HaTr 4, Tyndall et al. 2011b) than to the extended haloes found in some PNe (Corradi et al. 2003). Equatorial enhancements have been identified as prevalent in the morphologies of PNe with close-binary central stars, which could be indicative that the formation of the “halo” in Sp 1 is in some way connected with the shedding of the CE (as is suspected for more markedly toroidal structures, Miszalski et al. 2009b).

Sp 1 was found to be aligned approximately perpendicular to the plane of the central binary, consistent with theories of planetary nebula shaping by a close-binary central star. This is one of very few nebulae to have had this link explicitly shown (along with A 63: Mitchell et al. 2007, A 41: Jones et al. 2010b, NGC6337: Hillwig et al. 2010, A 65: Huckvale et al. 2011 and HaTr 4: Tyndall et al. 2011a,b), adding to the growing observational evidence that close-binary systems directly influence the morphological evolution of their host nebulae.

## 6 ACKNOWLEDGMENTS

We thank the anonymous referee for their swift and useful comments. We would also like thank Dr Alberto López, who obtained the AAT spectra and for useful discussions on the interpretation of the data. DJ thanks Dr. Todd Hillwig for several fruitful discussions about the central binary system of Sp 1, and María del Mar Rubio-Díez and Dr. Adam Avi-son for their assistance in the explication of the models.

We would like to thank the staff of the La Silla Paranal Observatory and the Anglo-Australian Telescope for their

support in the acquisition of the spectroscopic observations. This paper uses observations made at the South African Astronomical Observatory (SAAO).

## REFERENCES

- Balick B., 1987, *AJ*, 94, 671
- Balick B., Frank A., 2002, *A&A Annual Review*, 40, 439
- Bertin E., 1997, *SExtractor User’s Manual*. Institut de Astrophysique & Observatoire de Paris
- Bond H.E., Livio M., 1990, *ApJ*, 335, 568
- Bodman E. H. L., Schaub S. C., Hillwig T., 2011, *Journal of the Southeastern Association for Research in Astronomy*, in press
- Bryce M., Balick B., Meaburn J., 1994, *MNRAS*, 266, 721
- Corradi, R. L. M., Sabin, L., Miszalski, B., Rodríguez-Gil, P., Santander-García, M., Jones, D., Drew, J. E., Mampaso, A., Barlow, M. J., Rubio-Díez, M. M., Casares, J., Viironen, K., Frew, D. J., Giammanco, C., Greimel, R., & Sale, S. E. 2011, *MNRAS*, 410, 1349
- Corradi R.L.M., Schönberner D., Steffen M., Perinotto M., 2003, *MNRAS*, 340, 417
- de Marco O., 2009, *PASP*, 121, 316
- Dekker H., Delabre B., Dodorico S., 1986, In Crawford D.L., ed., *Society of Photo-Optical Instrumentation Engineers (SPIE) Conference Series*, vol. 627 of *Society of Photo-Optical Instrumentation Engineers (SPIE) Conference Series*, pp. 339–348
- Frew D., 2008, PhD Thesis, Macquarie University
- García-Díaz M.T., Clark D.M., López J.A., Steffen W., Richer M.G., 2009, *ApJ*, 699, 1633
- Gill C.D., O’Brien T.J., 1999, *MNRAS*, 307, 677
- Graham M.F., Meaburn J., López J.A., Harman D.J., Holloway A.J., 2004, *MNRAS*, 347, 1370
- Huckvale L., Prouse B., Jones D., Lloyd M., Pollacco D., 2011, In *Asymmetric Planetary Nebulae 5 Conference*, p. 113
- Hillwig T.C., Bond H.E., Afşar M., De Marco O., 2010, *AJ*, 140, 319
- Jones D., Lloyd M., Mitchell D.L., Pollacco D.L., O’Brien T.J., Vaytet N.M.H., 2010a, *MNRAS*, 401, 405
- Jones D., Lloyd M., Santander-García M., López J.A., Meaburn J., Mitchell D.L., O’Brien T.J., Pollacco D., Rubio-Díez M.M., Vaytet N.M.H., 2010b, *MNRAS*, 408, 2312
- Jones D., Tyndall A.A., Huckvale L., Prouse B., Lloyd M., 2011a, In Schmidtobreick L., Schreiber M.R., Tappert C., eds, *ASP Conf. Ser. Vol. 447, Evolution of Compact Binaries*. Astron. Soc. Pac., San Francisco, p. 165
- Jones D., Tyndall A.A., Lloyd M., Santander-García M., 2011b, In *IAUS 283: Planetary Nebulae: an Eye to the Future*, in press
- Kahn F.D., West K.A., 1985, *MNRAS*, 212, 837
- Kwok S., Purton C.R., Fitzgerald P.M., 1978, *ApJ*, 219, 125
- López J. A., Richer M. G., García-Díaz M. T., Clark D. M., Meaburn J., Riesgo H., Steffen W., Lloyd M., 2012, *RevMexAA*, 48, 3
- Meaburn J., Boumis P., López J.A., Harman D.J., Bryce M., Redman M.P., Mavromataki F., 2005, *MNRAS*, 360, 963

- Meaburn J., López J.A., Boumis P., Lloyd M., Redman M.P., 2009, *A&A*, 500, 827
- Meatheringham S.J., Wood P.R., Faulkner D.J., 1988, *ApJ*, 334, 862
- Méndez R.H., Kudritzki R.P., Herrero A., Husfeld D., Groth H.G., 1988, *A&A*, 190, 113
- Miszalski B., Acker A., Moffat A.F.J., Parker Q.A., Udalski A., 2009a, *A&A*, 496, 813
- Miszalski B., Acker A., Parker Q.A., Moffat A.F.J., 2009b, *A&A*, 505, 249
- Miszalski B., Corradi R. L. M., Boffin H. M. J., Jones D., Sabin L., Santander-García M., Rodríguez-Gil P., Rubio-Díez M. M., 2011a, *MNRAS*, 413, 1264
- Miszalski B., Jones D., Rodríguez-Gil P., Boffin H. M. J., Corradi R. L. M., Santander-García M., 2011b, *A&A*, 531, 158
- Mitchell D.L., Pollacco D., O'Brien T.J., Bryce M., Lopez J.A., Meaburn J., Vaytet N.M.H., 2007, *MNRAS*, 374, 1404
- Nordhaus J., Blackman E.G., 2006, *MNRAS*, 370, 2004
- Nordhaus J., Blackman E.G., Frank A., 2007, *MNRAS*, 376, 599
- Pollacco D.L., Bell S.A., 1993, *MNRAS*, 262, 377
- Pollacco D.L., Bell S.A., 1994, *MNRAS*, 267, 452
- Sabbadin F., 1986, *A&AS*, 64, 579
- Santander-García M., Rodríguez-Gil P., Jones D., Corradi R. L. M., Miszalski B., Pyrzas S., Rubio-Díez M. M., 2011, in *Asymmetric Planetary Nebulae 5*, edited by Zijlstra, A. A. and McDonald, I. and Lagadec, E., *Asymmetric Planetary Nebulae*, 259
- Shapley H., 1936, *Harvard College Observatory Bulletin*, 902, 26
- Smith N., Bally J., Walawender J., 2007, *AJ*, 134, 846
- Tyndall A.A., Jones D., Lloyd M., O'Brien T.J., Pollacco D.L., Mitchell D.L., 2011a, In *Asymmetric Planetary Nebulae 5 Conference*, p. 115
- Tyndall A.A., Jones D., Lloyd M., 2011b, In *IAUS 283: Planetary Nebulae: an Eye to the Future*, in press
- Wareing C.J., Zijlstra A.A., O'Brien T.J., 2007, *MNRAS*, 382, 1233
- Wilson R.E., Devinney E.J., 1971, *ApJ*, 166, 605